Finite-Time Robust Admissible Consensus Control of Multirobot System Under Dynamic Events

Anuj Nandanwar, Narendra Kumar Dhar, Dmitry Malyshev, Larisa Rybak, and Laxmidhar Behera

***Abstract*—This article addresses the problem of event-based consensus in a leader–follower multiagent system framework prone to external bounded disturbance. The proposed approach has three parts. The first part defines a novel measurement error based on sliding surface for super-twisting sliding-mode controller. The Lyapunov stability analysis is then used to derive a dynamic event-triggering condition for control updates. The event-based control updates guarantee stability along with the desired consensus amongst agents (robots). The second part derives a bound on reaching time to the sliding surface, thereby guaranteeing finite-time consensus control for each agent. The third part guarantees the admissibility of event-based control updates for each agent. The robustness of the proposed approach is validated through simulation and real-time experiments using three Pioneer P3-DX mobile robots in a multiagent framework. The real-time experimental results prove the reduction in computational burden of the entire system as control updates for two followers are found to be approximately 28.33% and 23.33%, respectively, in the presence of disturbances.**

***Index Terms*—Admissibility, consensus control, event-trigger, Lyapunov stability, sliding-mode control.**

I. Introduction

In THE recent two decades, distributed cooperative control and consensus problem for multiagent systems (MASs) [1] have garnered large attraction because of their wide-spread application in various areas such as area coverage and exploration, search and rescue mission [2], synchronization [3], and distributed optimization. Numerous works have been proposed related to consensus of MAS such as heterogeneous linear agent [3], first-order consensus with communication time-delay [4], second-order consensus [5], and nonholonomic system [6]. A very popular approach to achieve consensus has been artificial potential function [5]. It has some limitations [7]: a) local minima leading to traps, b) no way out when obstacles are nearby, c) oscillations occurring near obstacles and narrow spaces, and d) cannot reach the goal if obstacles are near. The work in [4] is simple, robust to time-delays during communication, and easy to implement in real-time applications. The common feature of [3]–[7] is that they consider continuous communication between the neighboring agents. The update of control inputs occur at each sampling instant. During real-time application, continuous communication and computational resources are important concerns for multiagent systems.

The event-based control scheme [8], [9] is an effective way to reduce the resource consumption in such system. Event-based controllers generate control input in aperiodic manner based on certain rule(s) or condition(s). In [10], an event-triggered controller has been developed for linear stochastic system of first-order. Based on distributed events, a self-triggered approach has been used to save energy for the system [11]. Dimarogonas *et al.* [12] have presented a preliminary work on event-based controller for MAS. The event-triggering strategy is applied to handle the problem of consensus in MAS with agents having single-integrator dynamics [13], general linear model [14], and second-order system dynamics [15]. Zhu and Jiang [16] addressed the consensus problem among leader–follower with general linear model and input delay, whereas Yu *et al.* [17] investigated the consensus problem in leader–follower framework using event-triggering for discrete first- and second-order systems with packet losses and time-varying delay. The major drawback of all these works is that they show consensus asymptotically but do not guarantee it in finite-time.

The event-based consensus of leader–follower and leaderless MAS in finite-time has been presented in [18]. The work in [19] studies time-triggered formation control of MAS in finite-time with nonholonomic robots as agents. The works [18] and [19] do not consider the effect of disturbance. An event-based H_∞ control is designed for consensus of discrete time-varying MAS with external disturbance [20]. This approach does not guarantee consensus in finite-time.

The sliding-mode control (SMC) is a very popular robust control technique and it rejects bounded disturbances and matched uncertainties. The second-order SMC (SOSMC) very efficiently fulfills this purpose. It belongs to the class of higher order SMC (HOSMC). One such controller is super-twisting SMC (STSMC) [21]. This approach steers the sliding variable to zero without using its time derivative for systems with relative degree of two. The approach proposed in [22] shows exponential convergence for linear systems, whereas there is no guarantee of finite-time convergence for higher order systems as the SOSMC

Manuscript received October 6, 2019; revised January 31, 2020; accepted February 29, 2020. This work was supported in part by the Department of Science and Technology of India under the research project DST-EE-2018309 and in part by the Russian Foundation for Basic Research under the research project 18-57-45014 IND_a. *(Corresponding author: Anuj Nandanwar.)*

Anuj Nandanwar, Narendra Kumar Dhar, and Laxmidhar Behera are with the Department of Electrical Engineering, Indian Institute of Technology Kanpur, Kanpur 208016, India (e-mail: anujnand@iitk.ac.in; nardhar@iitk.ac.in; lbehera@iitk.ac.in).

Dmitry Malyshev and Larisa Rybak are with the Department of Mechanical Engineering, Belgorod State Technological University, Belgorod 308012, Russian Federation (e-mail: dimon-belgorod@yandex.ru; rlbgtu@gmail.com).

Digital Object Identifier 10.1109/JSYST.2020.2979271

algorithm lacks local lipschitzness at origin. The SMC approach [23] handles tracking problem in finite-time for systems showing lipschitzness in their dynamics and prone to external disturbances. An integral SMC approach achieves consensus in finite-time for distributed second-order MAS with bounded disturbances [24]. Liu *et al.* [25] proposed a second-order super-twisting algorithm for the leader–follower MAS with system uncertainties and external disturbances. Yang *et al.* [26] proposed a methodology which is simple to design and reduces the computational burden during practical applications. It guarantees finite-time reachability and fault identification during operation even in the presence of stochastic noise, disturbance in output, and time delays. The simultaneous reconstructions of faults and states are achieved using reduced-order sliding-mode observer for time-delayed Markovian jump systems in [27]. Apart from simultaneous reconstructions, the methodology in [28] annuls the switching issue of sliding surfaces and avoids the necessity of reachability assay. All these works follow time-triggered approaches.

An event-based SMC technique seems to be the best-suited approach for disturbance rejection as well as reduction in communication and computational cost in a complex MAS. It is very difficult to derive a triggering strategy for finite-time consensus in the presence of nonlinear consensus protocol. For this, Behera and Bandhopadhay [29] assumed a nonlinear function in the locally Lipschitz continuous-time system dynamics with a unique equilibrium point. Nair *et al.* [30] have proposed an event-based integral SMC for multirobot consensus but the events for control updates are obtained through static threshold. As compared to HOSMC, integral SMC in [30] ignores the reaching phase. It forces the entire system response to pass through sliding mode. Though it reduces the sliding function to zero, it cannot do so with the derivatives of higher order. It cannot guarantee all the states to be finite-time stable. The other limitation of [30] is the chattering phenomena due to discontinuities generated by the control law. Though the approach in [31] considers heterogeneous agents for leader-tracking problem using dynamic controller, the triggering rule is again a static one. The transmission of information is affected by time-varying communication delays. The approach in [32] investigates dynamic event-triggered leader–follower consensus problem with matched and unmatched disturbances using traditional sliding-mode controller in finite-time. The approach does not consider HOSMC. Apart from this, an infinite number of switching occurs in finite time, i.e., Zeno behavior [33], a major issue to be taken care of in an event-based technique. To solve this problem, the control protocol should ensure that the interevent intervals have a strictly positive lower bound value. Wang *et al.* [34] devised an approach for consensus of asynchronously distributed MAS. It is a periodic event-based strategy which effectively removes Zeno behavior during sampling of data.

Motivated by the aforementioned discussion, the work presented in this article aims to design and implement an event-triggered STSMC for finite-time robust consensus in MAS prone to disturbances. The controller is applied to a real-time leader–follower MAS framework. In summary, this article has the following contributions:

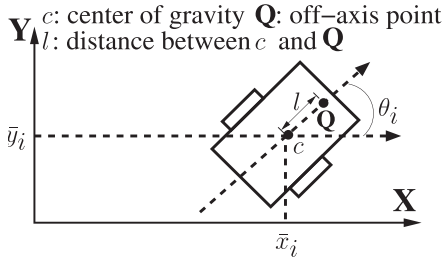

Fig. 1. Schematic of robot model.

1) design of dynamic event-based STSMC methodology for consensus in MAS;
2) the guarantee of finite-time consensus and stability of MAS;
3) the guarantee of lower bound on interevent execution time for admissibility of control updates; and
4) the real-time desired consensus in leader-follower framework with directed graph topology.

The rest of this article is organized as follows. The preliminaries and problem formulation are given in Section II. Section III has three subsections. The first one derives dynamic event-triggering condition. The second and third subsections present finite-time consensus and admissibility of event-based control, respectively. Section IV presents simulations, real-time experiments, and comparative analyses. The conclusions are drawn in Section V.

II. Preliminaries and Problem Formulation

A. Multiagent System Framework

A distributed MAS framework is considered for p robots as agents. These agents have single-integrator dynamics. They can interact and transmit data among each other. The communication topology between them is assumed to be a directed and weighted graph devoid of self-loops, $\mathcal{G} = (\mathcal{V}, \mathcal{E}, \mathcal{A})$ [30].

Notation: For any vector $\varepsilon = [\varepsilon_1, \varepsilon_2, \ldots, \varepsilon_n]^T$, a) $\text{sgn}(\varepsilon) = [\text{sgn}(\varepsilon_1), \text{sgn}(\varepsilon_2), \ldots, \text{sgn}(\varepsilon_n)]^T$, b) $|\varepsilon|^\eta = [|\varepsilon_1|^\eta, \ldots, |\varepsilon_n|^\eta]^T$, and c) $|\varepsilon|^\eta \text{sgn}(\varepsilon) = [|\varepsilon_1|^\eta \text{sgn}(\varepsilon_1), \ldots, |\varepsilon_n|^\eta \text{sgn}(\varepsilon_n)]^T$. The parameter $\eta \in \mathcal{R}$. The norm used in the article is defined as $||\varepsilon|| = \sqrt{\varepsilon^T \varepsilon}$.

B. System Dynamics and Control Input

The nonholonomic mobile robots in the MAS framework move on a $\mathbf{X}$–$\mathbf{Y}$ plane. Each agent of the group has the same built and dynamics. The kinematic model of any agent i as per Fig. 1 is similar to [35]

$$\dot{\bar{x}}_i = v_i \cos(\theta_i), \quad \dot{\bar{y}}_i = v_i \sin(\theta_i), \quad \dot{\theta}_i = \omega_i \tag{1}$$

where $\bar{\text{x}}_i = [\bar{x}_i \ \bar{y}_i]^T$ and θ_i represent position vector and turn angle, respectively. v_i and ω_i are linear and angular velocities, respectively.

An off-axis point $\mathbf{Q}$ is considered as the point of operation for robot i. The kinematic model (1) is first transformed to single-integrator form. The off-axis point is located at (x_i, y_i), where $x_i = \bar{x}_i + l\cos(\theta_i)$ and $y_i = \bar{y}_i + l\sin(\theta_i)$ with distance

l between center of gravity and $\mathbf{Q}$. The agent dynamics based on off-axis point is

$$\dot{x}_i = v_i \cos\theta_i - l\omega_i \sin\theta_i$$
$$\dot{y}_i = v_i \sin\theta_i + l\omega_i \cos\theta_i. \tag{2}$$

The linear and angular velocities are defined as

$$v_i = u_{ix}\cos\theta_i + u_{iy}\sin\theta_i$$
$$\omega_i = (-1/l)(u_{ix}\sin\theta_i - u_{iy}\cos\theta_i) \tag{3}$$

where $\mathrm{u}_i = [u_{ix}\, u_{iy}]^T$ is the control input vector generating these velocities. On using (3), (2) is simplified as

$$\dot{x}_i = u_{ix} \quad \dot{y}_i = u_{iy}. \tag{4}$$

The robot is prone to external disturbances (d_{ix}, d_{iy}). Hence, the dynamics (4) on incorporating the disturbance becomes

$$\dot{x}_i = u_{ix} + d_{ix} \quad \dot{y}_i = u_{iy} + d_{iy}. \tag{5}$$

The dynamics (5) can be written compactly in the single-integrator model form as

$$\dot{\mathrm{x}}_i = \mathrm{u}_i + d_i \tag{6}$$

where $\mathrm{x}_i = [x_i, y_i]^T$ and $d_i = [d_{ix}, d_{iy}]^T$ represent position vector and lumped uncertainty for external disturbances and unmodeled dynamics, respectively. The control input u_i for agent i is computed using event-based STSMC proposed in Section III.

The leader and follower robot dynamics in MAS framework based on (6) are therefore defined as

$$\dot{\mathrm{x}}_i(t) = \mathrm{u}_i(t) + d_i(t), \quad i = 1 \ldots p$$
$$\dot{\mathrm{x}}_0(t) = \mathrm{u}_0(t) \tag{7}$$

where $\mathrm{x}_i(t) \in \mathcal{R}^n, \mathrm{u}_i(t) \in \mathcal{R}^n$, and $\mathrm{d}_i(t) \in \mathcal{R}^n$ represent position, control input, and bounded disturbance, respectively of the ith follower robot. $\mathrm{x}_0(t) \in \mathcal{R}^n$ and $\mathrm{u}_0(t) \in \mathcal{R}^n$ are position and control input, respectively, of leader robot. The leader dynamics is assumed to be not affected by disturbance. Let $\tilde{\mathrm{x}}_i(t) = \mathrm{x}_i(t) - \mathrm{x}_0(t) + \Delta_i$ and $\tilde{\mathrm{u}}_i(t) = \mathrm{u}_i(t) - \mathrm{u}_0(t)$ be the deviations in position and control input of follower i from the leader, respectively. Δ_i is the desired position separation of follower i from leader. The relative dynamics of agent i based on the above deviations and (7) can be presented as

$$\dot{\tilde{\mathrm{x}}}_i(t) = \tilde{\mathrm{u}}_i(t) + d_i. \tag{8}$$

The STSMC sliding surface defined for an agent i in the MAS framework is

$$\mathrm{S}_i(t) = \tilde{\mathrm{x}}_i(t) - \int_0^t q_i^{\alpha}(t)dt, \quad i = 1 \ldots n \tag{9}$$

where

$$q_i(t) = -\frac{\gamma_i}{p_i+1}\sum_{j\in p_i} a_{ij}\{(\mathrm{x}_i(t) - \mathrm{x}_0(t) + \Delta_i) - (\mathrm{x}_j(t) - \mathrm{x}_0(t) + \Delta_j)\} + b_i(\mathrm{x}_i(t) - \mathrm{x}_0(t) + \Delta_i))$$
$$= -\frac{\gamma_i}{p_i+1}\sum_{j\in p_i} a_{ij}(\tilde{\mathrm{x}}_i(t) - \tilde{\mathrm{x}}_j(t)) + b_i\tilde{\mathrm{x}}_i(t). \tag{10}$$

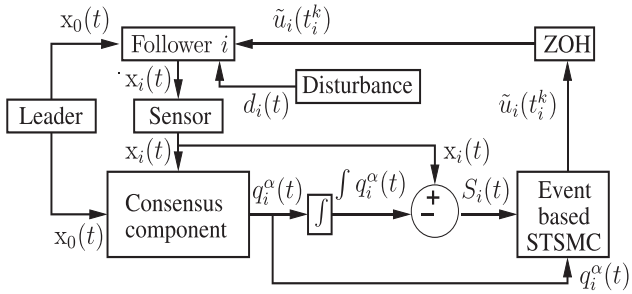

Fig. 2. Block schematic of the proposed approach.

$\mathrm{S}_i(t) = [s_1(t), s_2(t), \ldots s_n(t)]^T$ and q_i is the consensus component in (9). $\alpha \in (0,1)$ determines the rate of consensus, γ_i $(\gamma_i > 0)$ is a constant parameter, a_{ij} and b_i are the connection weights between the agents, and p_i $(1 \le p_i < p)$ is the number of agents neighboring to ith agent. With the onset of sliding phase, $S_i(t) = 0$. To achieve the desired consensus, we have considered a super-twisting control law

$$\tilde{\mathrm{u}}_i(t) = q_i^{\alpha}(t) - \mathrm{K}_1|\mathrm{S}_i(t)|^{\frac{1}{2}}\mathrm{sgn}(\mathrm{S}_i(t)) + \varrho_i(t)$$
$$\text{where} \quad \dot{\varrho}_i(t) = -\mathrm{K}_2\mathrm{sgn}(\mathrm{S}_i(t)). \tag{11}$$

The gain matrices $\mathrm{K}_1 = \mathrm{diag}\{k_{11}, k_{12}, \ldots, k_{1n}\}$ and $\mathrm{K}_2 = \mathrm{diag}\{k_{21}, k_{22}, \ldots, k_{2n}\}$, with each of their elements being positive gains. The control law $\tilde{\mathrm{u}}_i(t)$ in (11) is updated only at events (described in Section-III) and it remains the same until the next event triggers. The control law $\forall\, t\ (t_k^i \le t < t_{k+1}^i)$ is

$$\tilde{\mathrm{u}}_i(t) = q_i^{\alpha}(t_k^i) - \mathrm{K}_1|\mathrm{S}_i(t_k^i)|^{\frac{1}{2}}\mathrm{sgn}(\mathrm{S}_i(t_k^i)) + \varrho_i(t_k^i) \tag{12}$$

where t_k^i is the latest event instant.

Remark 1: The superscript $(i = 1, \ldots, p)$ and subscript $(k = 1, 2, \ldots)$ in t_k^i are agent and event number, respectively. ■

A novel measurement error (event-triggered error) e_i for each agent i has been defined to derive the event-triggering condition. The event-triggered error is defined as

$$e_i(t) = |S_i(t)|^{\frac{1}{2}}\mathrm{sgn}(S_i(t)) - |S_i(t_k^i)|^{\frac{1}{2}}\mathrm{sgn}(S_i(t_k^i))$$
$$= \begin{bmatrix} |s_1^i(t)|^{\frac{1}{2}}\mathrm{sgn}(s_1^i(t)) - |s_1^i(t_k^i)|^{\frac{1}{2}}\mathrm{sgn}(s_1^i(t_k^i)) \\ \vdots \\ |s_n^i(t)|^{\frac{1}{2}}\mathrm{sgn}(s_n^i(t)) - |s_n^i(t_k^i)|^{\frac{1}{2}}\mathrm{sgn}(s_n^i(t_k^i)) \end{bmatrix} \tag{13}$$

where $S_i(t)$ and $S_i(t_k^i)$ are sliding surfaces at current instant (t) and latest event-instant (t_k^i), respectively.

Using (8), (9), and (12), the surface dynamics $\forall\, t\ (t_k^i \le t < t_{k+1}^i)$ is

$$\dot{\mathrm{S}}_i(t) = q_i^{\alpha}(t_k^i) - \mathrm{K}_1|\mathrm{S}_i(t_k^i)|^{\frac{1}{2}}\mathrm{sgn}(\mathrm{S}_i(t_k^i)) + \varrho_i(t_k^i) + d_i - q_i^{\alpha}(t). \tag{14}$$

A schematic of the proposed approach is shown in Fig. 2. The event-based STSMC block first verifies whether event-triggering occurs or not. If yes, it then transmits control input $\tilde{u}_i$ to agent i. The ZOH (zero-order hold) block holds the control input until the next transmission occurs. The sampling time of ZOH is the same as that for the system operation. The following three assumptions have been considered while deriving the event-based control input.

Assumption 1: For the agent dynamics (7), the unmodeled dynamics/disturbance lumped together as d_i is assumed to be bounded, i.e., $d_i \leq \delta |S_i|^{\frac{1}{2}} \text{sgn}(S_i)$, where $\delta \in \mathcal{R}$.

Assumption 2: The difference $\Delta q_i = (q_i^\alpha(t_k^i) - q_i^\alpha(t))$ $\forall\, t\ (t_k^i \leq t < t_{k+1}^i)$ is bounded as $\Delta q_i \leq \Phi_i$ where $\Phi_i \in \mathcal{R}$.

Assumption 3: The event-triggered error magnitude $\forall\, t\ (t_k^i \leq t < t_{k+1}^i)$ of any agent i is bounded as $\|e_i\| \leq e_{tr}$.

Remark 2: The consensus component q_i is defined using the difference of position of agents which change finitely based on velocity inputs. Hence, Δq_i in Assumption 2 is considered to be bounded in interevent duration. The event-triggered error depends on difference of sliding surfaces as per (13). The magnitude of this difference is finite for interevent duration and hence validates Assumption 3. ■

C. Problems

The solution to the following three problems are integral to the design of the proposed finite-time robust admissible consensus control in the presence of external bounded disturbance.

Problem 1: Given the agent dynamics (7), derive the dynamic event-triggering condition for each agent i such that the event-based control input from STSMC achieves consensus and renders the system stable.

Problem 2: Guarantee the finite-time consensus by having finite reaching time to the sliding surface for each agent?

Problem 3: Guarantee the admissibility of event-based control law for each agent?

The solutions have been presented in the following section.

III. Event-Triggered Consensus Control

The proposed methodology has three parts. The first part derives the dynamic event-triggering condition necessary for updating control inputs of respective agents in the MAS. The second part guarantees finite reaching time to the sliding surface while the third part guarantees admissibility of event-based control.

A. Event-Triggering Condition

Theorem 1 presents event-triggering condition required for control input updates of agents. The approach will ensure consensus among agents and their stability.

Theorem 1: Consider the dynamics of agent i (7) with its event-based control law (12). If the condition

$$\|e_i\| > \left\| z_2 - |S_i(t_k^i)|^{\frac{1}{2}} \text{sgn}(S_i(t_k^i)) \right\|$$
$$\text{where} \quad z_2 = \frac{-\kappa + \sqrt{\kappa^2 - 4\beta\rho}}{2\beta} \tag{15}$$

is satisfied, then an event triggers and control input for the agent i is updated at that instant. The gradual events result in its consensus with other agents of MAS in the presence of disturbance and further ensure stability.

Proof: The Lyapunov function considered for the agent i is

$$V_i = \zeta_i^T P_i \zeta_i \tag{16}$$

where $\zeta_i = \begin{bmatrix} |S_i|^{\frac{1}{2}} \text{sgn}(S_i) \\ \varrho_i \end{bmatrix}$ and $P_i = \frac{1}{2}\begin{bmatrix} 4K_2 + K_1^2 & -K_1 \\ -K_1 & 2I \end{bmatrix}$.

The time derivative of Lyapunov function in (16) is

$$\dot{V}_i = \dot{\zeta}_i^T P \zeta_i + \zeta_i^T P \dot{\zeta}_i \tag{17}$$

where $\dot{\zeta}_i = [\frac{1}{2}|S_i|^{-\frac{1}{2}}(\varphi_i + d_i) \quad -K_2 \text{sgn}(S_i)]^T$ and $\varphi_i = q_i^\alpha(t_k^i) - K_1 |S_i(t_k^i)|^{\frac{1}{2}} \text{sgn}(S_i(t_k^i))) + \varrho_i(t_k^i) - q_i^\alpha(t)$. The component $\dot{\zeta}_i^T P \zeta_i$ in (17) is

$$\begin{aligned}
\dot{\zeta}_i^T P \zeta_i &= \begin{bmatrix} \frac{1}{2}|S_i|^{-\frac{1}{2}}(\varphi_i + d_i) & -K_2 \text{sgn}(S_i) \end{bmatrix} \\
&\quad \times \frac{1}{2}\begin{bmatrix} 4K_2 + K_1^2 & -K_1 \\ -K_1 & 2I \end{bmatrix} \begin{bmatrix} |S_i|^{\frac{1}{2}} \text{sgn}(S_i) \\ \varrho_i \end{bmatrix} \\
&= \frac{1}{2}\begin{bmatrix} \frac{1}{2}|S_i|^{-\frac{1}{2}}(\varphi_i + d_i) & -K_2 \text{sgn}(S_i) \end{bmatrix} \\
&\quad \begin{bmatrix} 4K_2|S_i|^{\frac{1}{2}} \text{sgn}(S_i) + K_1^2 |S_i|^{\frac{1}{2}} \text{sgn}(S_i) - K_1 \varrho_i \\ -K_1 |S_i|^{\frac{1}{2}} \text{sgn}(S_i) + 2\varrho_i \end{bmatrix} \\
&= \frac{1}{4}|S_i|^{-\frac{1}{2}} \Big[(\varphi_i + d_i)(4K_2 |S_i|^{\frac{1}{2}} \text{sgn}(S_i) \\
&\quad + K_1^2 |S_i|^{\frac{1}{2}} \text{sgn}(S_i) - K_1 \varrho_i) + 2K_1 K_2 |S_i| \\
&\quad - 4K_2 \varrho_i |S_i|^{\frac{1}{2}} \text{sgn}(S_i) \Big].
\end{aligned} \tag{18}$$

Similarly, the component $\zeta_i^T P \dot{\zeta}_i$ of $\dot{V}_i$ is

$$\begin{aligned}
\zeta_i^T P \dot{\zeta}_i &= \begin{bmatrix} |S_i|^{\frac{1}{2}} \text{sgn}(S_i) & \varrho_i \end{bmatrix} \\
&\quad \times \frac{1}{2}\begin{bmatrix} 4K_2 + K_1^2 & -K_1 \\ -K_1 & 2I \end{bmatrix} \begin{bmatrix} \frac{1}{2}|S_i|^{-\frac{1}{2}}(\varphi_i + d_i) \\ -K_2 \text{sgn}(S_i) \end{bmatrix} \\
&= \frac{1}{4}|S_i|^{-\frac{1}{2}} \Big[(\varphi_i + d_i)(4K_2 |S_i|^{\frac{1}{2}} \text{sgn}(S_i) \\
&\quad + K_1^2 |S_i|^{\frac{1}{2}} \text{sgn}(S_i) - K_1 \varrho_i) + 2K_1 K_2 |S_i| \\
&\quad - 4K_2 \varrho_i |S_i|^{\frac{1}{2}} \text{sgn}(S_i) \Big].
\end{aligned} \tag{19}$$

Using (18) and (19), (17) can be written as

$$\begin{aligned}
\dot{V}_i &= \frac{1}{2}|S_i|^{-\frac{1}{2}} \Big[\varphi_i (4K_2 |S_i|^{\frac{1}{2}} \text{sgn}(S_i) + K_1^2 |S_i|^{\frac{1}{2}} \text{sgn}(S_i) \\
&\quad - K_1 \varrho_i) + d_i (4K_2 |S_i|^{\frac{1}{2}} \text{sgn}(S_i) + K_1^2 |S_i|^{\frac{1}{2}} \text{sgn}(S_i) \\
&\quad - K_1 \varrho_i) + 2K_1 K_2 |S_i| - 4K_2 \varrho_i |S_i|^{\frac{1}{2}} \text{sgn}(S_i) \Big].
\end{aligned} \tag{20}$$

On applying disturbance bound as per Assumption 1 in (20)

$$\begin{aligned}
\dot{V}_i &\leq \frac{1}{2}|S_i|^{-\frac{1}{2}} \Big[4K_2 \varphi_i |S_i|^{\frac{1}{2}} \text{sgn}(S_i) + K_1^2 \varphi_i |S_i|^{\frac{1}{2}} \text{sgn}(S_i) \\
&\quad - K_1 \varphi_i \varrho_i + 4K_2 \delta |S_i| + K_1^2 \delta |S_i| - K_1 \varrho_i \delta |S_i|^{\frac{1}{2}} \text{sgn}(S_i) \\
&\quad + 2K_1 K_2 |S_i| - 4K_2 \varrho_i |S_i|^{\frac{1}{2}} \text{sgn}(S_i) \Big].
\end{aligned} \tag{21}$$

Let $z_i = |S_i|^{\frac{1}{2}} \text{sgn}(S_i)$. On expressing (21) in terms of z_i

$$\begin{aligned}
\dot{V}_i &\leq \frac{1}{2}|S_i|^{-\frac{1}{2}} \big[4K_2 \varphi_i z_i + K_1^2 \varphi_i z_i - K_1 \varphi_i \varrho_i + 4K_2 \delta z_i^2 \\
&\quad + K_1^2 \delta z_i^2 - K_1 \varrho_i \delta z_i + 2K_1 K_2 z_i^2 - 4K_2 \varrho_i z_i \big]
\end{aligned}$$

$$= \frac{1}{2}|S_i|^{-\frac{1}{2}}\left[z_i^2(4K_2\delta + K_1^2\delta + 2K_1K_2) + z_i(4K_2\varphi_i + K_1^2\varphi_i - K_1\varrho_i\delta - 4K_2\varrho_i) + (-K_1\varphi_i\varrho_i)\right]$$

$$= \frac{1}{2}|S_i|^{-\frac{1}{2}}\left[\beta z_i^2 + \kappa z_i + \rho\right] \tag{22}$$

where $\beta = 4K_2\delta + K_1^2\delta + 2K_1K_2$, $\kappa = 4K_2\varphi_i + K_1^2\varphi_i - K_1\varrho_i\delta - 4K_2\varrho_i$, and $\rho = -K_1\varrho_i\varphi_i$. For stability, $\dot{V}_i \leq 0$.

Hence

$$\frac{1}{2}|S_i|^{-\frac{1}{2}}\left[\beta z_i^2 + \kappa z_i + \rho\right] \leq 0$$

$$\Rightarrow \quad \beta z_i^2 + \kappa z_i + \rho \leq 0 \Rightarrow (z_i - z_1)(z_i - z_2) \leq 0$$

$$\text{where} \quad (z_1, z_2) = \frac{-\kappa \pm \sqrt{\kappa^2 - 4\beta\rho}}{2\beta}. \tag{23}$$

Remark 3: For z_1 and z_2 to have real values, $\kappa^2 - 4\beta\rho \geq 0$. This is ensured by the parameters considered for the agents. Let for agent i, $z_1 \leq z_2$. ■

Since $z_1 \leq z_2$, the sufficient condition for system stability is

$$(z_i - z_2) \leq 0 \Rightarrow z_i \leq z_2. \tag{24}$$

On substituting the expression for z_i in (24)

$$|S_i|^{\frac{1}{2}}\text{sgn}(S_i) \leq z_2. \tag{25}$$

From (13)

$$|S_i|^{\frac{1}{2}}\text{sgn}(S_i) = e_i + |S_i(t_k^i)|^{\frac{1}{2}}\text{sgn}(S_i(t_k^i)). \tag{26}$$

On rewriting (25) using (26)

$$e_i + |S_i(t_k^i)|^{\frac{1}{2}}\text{sgn}(S_i(t_k^i)) \leq z_2$$

$$\Rightarrow \; e_i \leq z_2 - |S_i(t_k^i)|^{\frac{1}{2}}\text{sgn}(S_i(t_k^i)). \tag{27}$$

The system is stable for the condition obtained in (27). The above condition can be further written as

$$\|e_i\| \leq \left\| z_2 - |S_i(t_k^i)|^{\frac{1}{2}}\text{sgn}(S_i(t_k^i)) \right\|. \tag{28}$$

Remark 4: The components on both sides of (27) are vector quantities. Hence, a simplified form is written in (28). ■

On the contrary, an event is triggered when

$$\|e_i\| > \left\| z_2 - |S_i(t_k^i)|^{\frac{1}{2}}\text{sgn}(S_i(t_k^i)) \right\|. \tag{29}$$

Equation (29) is therefore the event-triggering condition for agent i. All the agents will have similar condition like (29).

Remark 5: (a) Equation (29) presents a dynamic condition as the parameters on right-hand side (RHS) change value at different time instants. (b) For smooth implementation of (29) in real-time scenario, the "$>$" symbol is replaced by "$\geq$." ■

B. Finite-Time Consensus Control

For real-time consensus applications, the sliding phase should start in finite time, or, in other words, reaching time to the sliding surface should be finite. The describing point of an agent then moves along its sliding surface. Theorem 2 guarantees finite-time consensus control by STSMC.

Theorem 2: For the triggering condition (15) and the event-based control law (12), the reaching time T_r to the sliding surface is finite and upper bounded by

$$T_r = \frac{2}{\delta}\left[\left\| -|S_i(t_{S_0})|^{\frac{1}{2}}\text{sgn}(S_i(t_{S_0})) - \frac{\varsigma_i}{\delta}\ln\left(-\delta|S_i(t_{S_0})|^{\frac{1}{2}}\text{sgn}(S_i(t_{S_0}))\right)\right\|\right]. \tag{30}$$

Proof: From (9), the sliding surface dynamics can be given by

$$\dot{S}_i = \dot{\tilde{\text{x}}}_i - q_i^{\alpha}. \tag{31}$$

Equation (31) can be further written using (8) as

$$\dot{S}_i = \tilde{\text{u}}_i + d_i - q_i^{\alpha}. \tag{32}$$

On using the control input $\tilde{\text{u}}_i$ from (12) at $t = t_{S_0}$ in (32)

$$\dot{S}_i = q_i^{\alpha}(t_{S_0}) - K_1|S_i(t_{S_0})|^{\frac{1}{2}}\text{sgn}(S_i(t_{S_0})) + \varrho_i(t_{S_0}) + d_i - q_i^{\alpha} \tag{33}$$

where $S_i(t_{S_0})$ is the initial value (at $t = t_{S_0}$) when agent i starts toward the sliding surface. As per Assumptions 1 and 2, (33) can be expressed as

$$\dot{S}_i \leq \Phi_i - K_1|S_i(t_{S_0})|^{\frac{1}{2}}\text{sgn}(S_i(t_{S_0})) + \varrho_i(t_{S_0}) + \delta|S_i|^{\frac{1}{2}}\text{sgn}(S_i). \tag{34}$$

Let $\varsigma_i = \Phi_i - K_1|S_i(t_{S_0})|^{\frac{1}{2}}\text{sgn}(S_i(t_{S_0})) + \varrho_i(t_{S_0})$ for simplicity of expression. Inequality (34) can be written as

$$\dot{S}_i = \frac{dS_i}{dt} \leq \delta|S_i|^{\frac{1}{2}}\text{sgn}(S_i) + \varsigma_i. \tag{35}$$

The maximum rate of change of sliding surface is

$$\frac{dS_i}{dt} = \delta|S_i|^{\frac{1}{2}}\text{sgn}(S_i) + \varsigma_i. \tag{36}$$

Remark 6: Equation (36) has vector components on the left- and right-hand sides. To proceed further, L_2 norm has been used. ■

The maximum reaching time can therefore be obtained from (36) as

$$\left\| \int_{S_i(t_{S_0})}^{S_i(t_{S_f})} \frac{dS_i}{\delta|S_i|^{\frac{1}{2}}\text{sgn}(S_i) + \varsigma_i} \right\| = \int_{t_{S_0}}^{t_{S_f}} dt \tag{37}$$

where $S_i(t_{S_f})$ is the value (at $t = t_{S_f}$) when agent i reaches the sliding surface.

Remark 7: The $S(t_{S_0})$ and $S(t_{S_f})$ are values at time instants t_{S_0} and t_{S_f} when describing point of i^{th} agent initially starts toward and finally reaches the sliding surface, respectively. ■

On simplifying expression (37)

$$\frac{2}{\delta}\left[\left\| |S_i|^{\frac{1}{2}}\text{sgn}(S_i)\Big|_{S_i(t_{S_0})}^{S_i(t_{S_f})} - \frac{\varsigma_i}{\delta}\ln\left(\delta|S_i|^{\frac{1}{2}}\text{sgn}(S_i) + \varsigma_i\Big|_{S_i(t_{S_0})}^{S_i(t_{S_f})}\right)\right\|\right] = t_{S_f} - t_{S_0}. \tag{38}$$

As the agent reaches sliding surface, the value of S_i, i.e., $S(t_{S_f}) = 0$. Equation (38) is further expressed as

$$\frac{2}{\delta}\Bigg[\Bigg| - |S_i(t_{S_0})|^{\frac{1}{2}}\text{sgn}(S_i(t_{S_0})) - \frac{\varsigma_i}{\delta}\ln\left(-\delta|S_i(t_{S_0})|^{\frac{1}{2}}\text{sgn}(S_i(t_{S_0}))\right)\Bigg|\Bigg] = (t_{S_f} - t_{S_0}) \quad (39)$$

where $t_{S_f} - t_{S_0} = T_r$. On rearranging (39)

$$T_r = \frac{2}{\delta}\Bigg[\Bigg| - |S_i(t_{S_0})|^{\frac{1}{2}}\text{sgn}(S_i(t_{S_0})) - \frac{\varsigma_i}{\delta}\ln\left(-\delta|S_i(t_{S_0})|^{\frac{1}{2}}\text{sgn}(S_i(t_{S_0}))\right)\Bigg|\Bigg]. \quad (40)$$

The T_r in (40) is the maximum reaching time to the sliding surface.

C. Admissibility of Event-Based Control

The admissibility of event-triggered control is necessary to avoid the piling of triggering instants (i.e., Zeno effect) which can force the system to instability. Theorem 3 provides a bound on interevent execution duration to avoid such scenario.

Theorem 3: For the system in (7), event-based control is updated when the condition in (15) is satisfied. The admissibility of such control update is guaranteed if the interevent execution time T_e ($T_e = t^i_{k+1} - t^i_k$) is lower bounded by

$$T_e \geq 2\left\||S_i(t^i_k)|^{\frac{1}{2}}\right\|\ln\left(1 + \frac{\delta e_{tr}}{\left\|\delta|S_i(t^i_k)|^{\frac{1}{2}}\text{sgn}(S_i(t^i_k)) + \varsigma_i\right\|}\right). \quad (41)$$

Proof: The event-triggered error for agent i is

$$e_i = |S_i(t)|^{\frac{1}{2}}\text{sgn}(S_i(t)) - |S_i(t^i_k)|^{\frac{1}{2}}\text{sgn}(S_i(t^i_k)). \quad (42)$$

The time derivative of event-triggered error in (42) is

$$\dot{e}_1 = \frac{d}{dt}\left(|S_i(t)|^{\frac{1}{2}}\text{sgn}(S_i(t)) - |S_i(t^i_k)|^{\frac{1}{2}}\text{sgn}(S_i(t^i_k))\right) = \frac{1}{2}|S_i|^{-\frac{1}{2}}\dot{S}_i. \quad (43)$$

Substituting $\dot{S}_i$ from (32) in (43) gives

$$\dot{e}_i = \frac{1}{2}|S_i|^{-\frac{1}{2}}(q^\alpha_i(t^i_k) - K_1|S_i(t^i_k)|^{\frac{1}{2}}\text{sgn}(S_i(t^i_k)) + \varrho_i(t^i_k) + d_i - q^\alpha_i). \quad (44)$$

Using Assumptions 1 and 2 in (44)

$$\dot{e}_i \leq \frac{1}{2}|S_i|^{-\frac{1}{2}}\left(\Phi_i - K_1|S_i(t^i_k)|^{\frac{1}{2}}\text{sgn}(S_i(t^i_k)) + \varrho_i(t^i_k) + \delta|S_i|^{\frac{1}{2}}\text{sgn}(S_i)\right). \quad (45)$$

Using $\varsigma_i = \Phi_i - K_1|S_i(t^i_k)|^{\frac{1}{2}}\text{sgn}(S_i(t^i_k)) + \varrho_i(t^i_k)$ the same as in Section III-B, inequality (45) is written as

$$\dot{e}_i \leq \frac{1}{2}|S_i|^{-\frac{1}{2}}\left(\delta|S_i|^{\frac{1}{2}}\text{sgn}(S_i) + \varsigma_i\right). \quad (46)$$

Using (42) and (46) is written in terms of event-triggered error as

$$\dot{e}_i = \frac{d(e_i)}{dt} \leq \frac{1}{2}|S_i(t^i_k)|^{-\frac{1}{2}}\left(\delta(e_i + |S_i(t^i_k)|^{\frac{1}{2}}\text{sgn}(S_i(t^i_k))) + \varsigma_i\right)$$

$$\Rightarrow \frac{d(e_i)}{dt} \leq \begin{bmatrix} \frac{1}{2}|s^i_1(t^i_k)|^{-\frac{1}{2}}\left(\delta(e^i_1 + |s^i_1(t^i_k)|^{\frac{1}{2}}\text{sgn}(s^i_1(t^i_k))) + \varsigma^i_1\right) \\ \vdots \\ \frac{1}{2}|s^i_n(t^i_k)|^{-\frac{1}{2}}\left(\delta(e^i_n + |s^i_n(t^i_k)|^{\frac{1}{2}}\text{sgn}(s^i_n(t^i_k))) + \varsigma^i_n\right) \end{bmatrix}. \quad (47)$$

Using the vector norm in (47), we can write

$$\frac{d\|e_i\|}{dt} \leq \frac{1}{2}\left\||S_i(t^i_k)|^{-\frac{1}{2}}\left(\delta(e_i + |S_i(t^i_k)|^{\frac{1}{2}}\text{sgn}(S_i(t^i_k))) + \varsigma_i\right)\right\|$$

$$\leq \frac{1}{2}\left\||S_i(t^i_k)|^{-\frac{1}{2}}\right\|\left(\delta\|e_i\| + \left\|\delta|S_i(t^i_k)|^{\frac{1}{2}}\text{sgn}(S_i(t^i_k)) + \varsigma_i\right\|\right). \quad (48)$$

From (48)

$$\int_0^{e_{tr}} \frac{d\|e_i\|}{\delta\|e_i\| + \left\|\delta|S_i(t^i_k)|^{\frac{1}{2}}\text{sgn}(S_i(t^i_k)) + \varsigma_i\right\|} \leq \int_{t^i_k}^{t^i_{k+1}} \frac{1}{2}\left\||S_i(t^i_k)|^{-\frac{1}{2}}\right\| dt$$

$$\Rightarrow \ln\left(\frac{\delta\|e_i\| + \left\|\delta|S_i(t^i_k)|^{\frac{1}{2}}\text{sgn}(S_i(t^i_k)) + \varsigma_i\right\|}{\delta}\right)\Bigg|_0^{e_{tr}} \leq \frac{1}{2}\left\||S_i(t^i_k)|^{-\frac{1}{2}}\right\| t\Big|_{t^i_k}^{t^i_{k+1}}. \quad (49)$$

As per Assumption 3, $\|e_i\| \leq e_{tr}$. On simplifying and rearranging (49)

$$\frac{1}{2}\left\||S_i(t^i_k)|^{-\frac{1}{2}}\right\|(t^i_{k+1} - t^i_k) \geq \ln\left(\frac{\delta e_{tr} + \left\|\delta|S_i(t^i_k)|^{\frac{1}{2}}\text{sgn}(S_i(t^i_k)) + \varsigma_i\right\|}{\left\|\delta|S_i(t^i_k)|^{\frac{1}{2}}\text{sgn}(S_i(t^i_k)) + \varsigma_i\right\|}\right)$$

$$\Rightarrow T_e \geq 2\left\||S_i(t^i_k)|^{\frac{1}{2}}\right\|\ln\left(1 + \frac{\delta e_{tr}}{\left\|\delta|S_i(t^i_k)|^{\frac{1}{2}}\text{sgn}(S_i(t^i_k)) + \varsigma_i\right\|}\right) \quad (50)$$

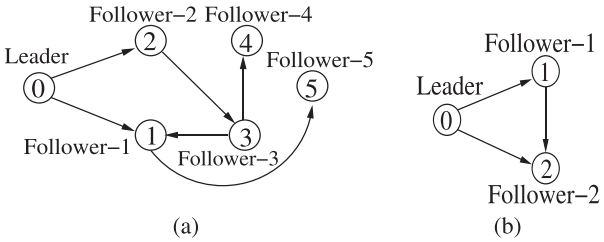

Fig. 3. MAS digraph for (a) simulation and (b) real-time experiment.

where $T_e = t^i_{k+1} - t^i_k$. The value of T_e obtained in (50) provides lower bound on interexecution time before the next event occurs.

Remark 8: The interevent time is defined using the last (t^i_k) and forthcoming event instant (t^i_{k+1}). Hence, S_i at $t = t^i_k$ and $t = t^i_{k+1}$ are considered. ■

Remark 9: Equation (47) has vector components on LHS and RHS. To proceed further, the vector norm has been used. ■

Remark 10: The value of T_e varies for different interevent duration as the parameters involved change their values. ■

IV. Case Study

The proposed methodology has been validated through simulation and real-time experiments.

Remark 11: In the experiments (simulation and real-time), we have considered random data packet losses and delays in the network. The data communication among the mobile robots in real-time experiment occurs through wireless network following IEEE 802.11 protocol which is susceptible to the above network uncertainties. ■

Remark 12: There are some limitations during implementations. In the experiments, only time-varying matched disturbances are considered. Only random packet losses and delays are considered as wireless network (following IEEE 802.11 protocol) is used, which is susceptible to network uncertainties. There is no separate fault identification and isolation module in the proposed model. ■

A. Simulation Experiment

The approach has been validated through simulation in Gazebo environment with Pioneer P3-DX robot model. In the MAS framework shown in Fig. 3 (a), five robots act as follower and one acts as leader. All robot models are identical in performance and control. Each robot system is equipped with an onboard computer with Ubuntu 14 platform having robot operating system (ROS), which facilitates an ultimate control over all sensors and actuators. A Wi-Fi router (Tinda) is used to maintain a sufficient network strength throughout the experiment. Each robot is provided a unique IP address for exchange of information with each other. The odometer sensor provides current position and orientation of mobile robot. The sensor data is available at the rate of 10 Hz. Hence, 0.01 s is used as sampling interval.

The weight for the communication among agents is assumed to be 1. As per the communication graph $\mathcal{G}$ in Fig. 3(a), the

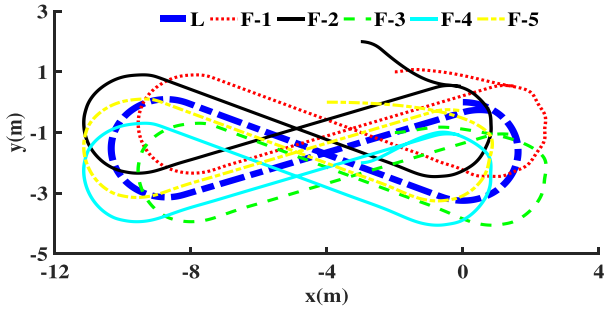

Fig. 4. Trajectory of robots during desired formation.

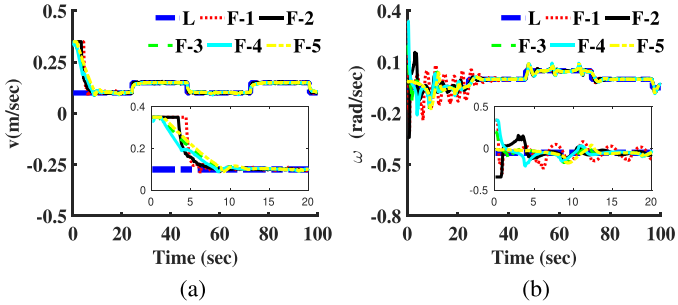

Fig. 5. (a) Linear velocity and (b) angular velocity of robots.

consensus parameters are

$$\mathcal{L} = \begin{bmatrix} 1 & 0 & -1 & 0 & 0 \\ 0 & 0 & 0 & 0 & 0 \\ 0 & -1 & 1 & 0 & 0 \\ 0 & 0 & -1 & 1 & 0 \\ -1 & 0 & 0 & 0 & 1 \end{bmatrix} \quad \mathcal{B} = \begin{bmatrix} 1 & 0 & 0 & 0 & 0 \\ 0 & 1 & 0 & 0 & 0 \\ 0 & 0 & 0 & 0 & 0 \\ 0 & 0 & 0 & 0 & 0 \\ 0 & 0 & 0 & 0 & 0 \end{bmatrix}.$$

The leader is free to move in any direction. The initial position of leader is $\mathrm{x}_0 = [0; 0]$, whereas followers are initially at $\mathrm{x}_1 = [-2; 1]$, $\mathrm{x}_2 = [-3; 2]$, $\mathrm{x}_3 = [-2; -1]$, $\mathrm{x}_4 = [-3; -2]$, and $\mathrm{x}_5 = [-4; 0]$. The system parameters are as follows: $l = 0.21\,\mathrm{m}$, $\mathrm{K}_1 = \mathrm{diag}\{0.5, 0.5\}$, $\mathrm{K}_2 = \mathrm{diag}\{0.001, 0.001\}$, $\Delta_1 = (-0.8\,\mathrm{m}, -0.8\,\mathrm{m})$, $\Delta_2 = (0.8\,\mathrm{m}, -0.8\,\mathrm{m})$, $\Delta_3 = (-0.8\,\mathrm{m}, 0.8\,\mathrm{m})$, $\Delta_4 = (0.8\,\mathrm{m}, 0.8\,\mathrm{m})$, $\Delta_5 = (0.8\,\mathrm{m}, 0\,\mathrm{m})$, and $\alpha = 5/7$. The parameter δ in disturbance bound as per Assumption 1 is 0.01.

The task is to achieve the shape of *Gerono lemniscate* (horizontally oriented eight-shaped figure). The leader and follower robots' trajectories are shown in Fig. 4. The leader pursues the trajectory-shaped Gerono lemniscate whereas followers follow the leader trajectory maintaining a desired distance. Initially, the robots are not in consensus but after few seconds, they gradually attain the desired trajectory. Fig. 5 shows the linear and angular velocities of followers with respect to the leader. It can be observed that the velocities of followers gradually get in sync with the leader velocities. Fig. 6(a) ensures that the desired separation is gradually maintained throughout the task even in the presence of disturbances. The sliding surfaces of all the follower agents are shown in Fig. 6(b). All the agents attain their respective desired sliding surface in finite-time. The dynamic

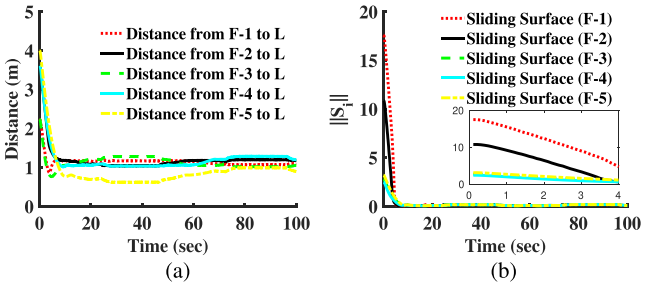

Fig. 6. (a) Relative distance of followers from leader and (b) sliding surface of followers.

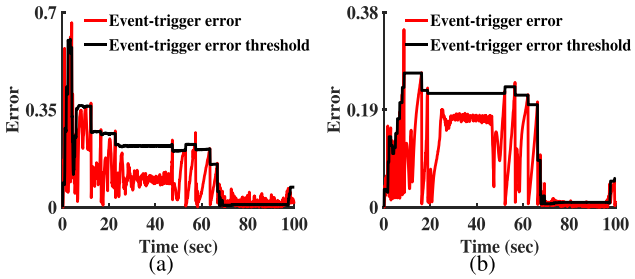

Fig. 7. Event-triggered error and threshold of (a) F-1 and (b) F-3.

TABLE I
EVENTS TRIGGERED FOR FOLLOWER ROBOTS

	F-1	F-2	F-3	F-4	F-5
Number of events	196	209	90	94	84
Events triggered (in %)	19.6	20.9	9	9.4	8.4

F: Follower.

event-triggered errors and their thresholds for F-1 and F-3 are shown in Fig. 7. The other agents too provide the similar results. The events occur when errors cross their respective dynamic thresholds. It can be observed that events are more when there are turns or change in orientations of the trajectory. Table I shows the number and percentage of events triggered for all the five follower robots during consensus in 100 s.

B. Real-Time Experiments

Three Pioneer P3-DX (two-wheeled differentially driven) robots have been used for real-time experiments which form a MAS framework. The two robots are followers while one acts as a leader. The robots are equipped with sonar sensor and position encoder. They communicate through wireless network having unique IP addresses assigned to them.

The consensus parameters of the graph are $\mathcal{L} = [0\ 0; -1\ 1]$ and $\mathcal{B} = [1\ 0; 0\ 1]$. The leader robot is free to roam in any direction. To achieve consensus-based formation, the followers should keep track of leader trajectory. The initial position of leader is $x_0 = [0; 0]$, whereas followers are initially at $x_1 = [-4; 0.5]$ and $x_2 = [-4; -0.5]$. The system parameters are as follows: $l = 0.21$ m, $K_1 = \text{diag}\{0.5, 0.5\}$, $K_2 = \text{diag}\{0.001, 0.001\}$, $\Delta_1 = (0.7\text{ m}, -0.7\text{ m})$, $\Delta_2 = (0.7\text{ m}, 0.7\text{ m})$, and $\alpha = 5/7$. The

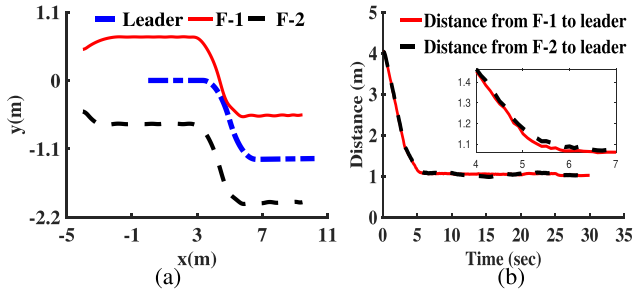

Fig. 8. (a) Trajectory of robots during desired formation. (b) Relative distance of followers from leader.

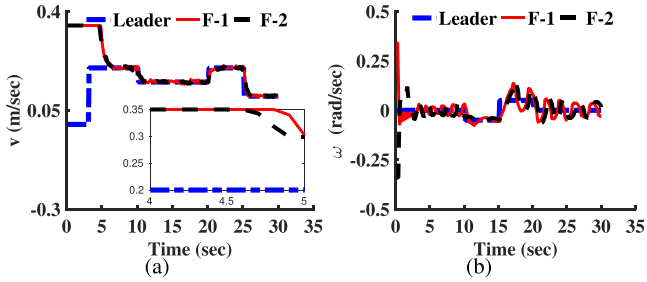

Fig. 9. (a) Linear velocity and (b) angular velocity of robots.

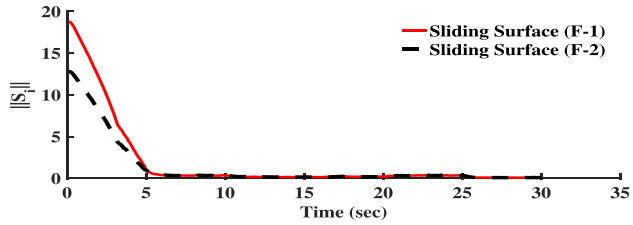

Fig. 10. Sliding surfaces of two followers.

sampling time considered for the experiments is 0.01 s. The value of δ in disturbance bound is 0.01.

The trajectories of all the robots are shown in Fig. 8(a). The desired formation is achieved for leader-follower framework as the desired deviation $\|\Delta\|$ is obtained in Fig. 8(b). The distance between each follower and leader is large initially but after some time event-based controllers drive the agents to a desired formation and then maintain required separations for rest of the trajectory. The linear and angular velocities of the robots are shown in Fig. 9(a) and (b), respectively. The proposed controller has been tested for various velocities and turn maneuvers. The sliding surfaces ($\|S\|$) of the followers are presented in Fig. 10. The result suggests that the describing point of agents reach the sliding surfaces approximately in 12.3 s. The expression of upper bound on finite reaching time in (40) evaluates to 115.94 s. Thus, the reaching time during real-time experiment is well below the upper bound. The event-triggered error and the respective error threshold as per condition in (15) for both the followers are shown in Fig. 11. The event-triggered error crosses the threshold very frequently initially which leads to triggering of events for control update. As the consensus is gradually achieved, the

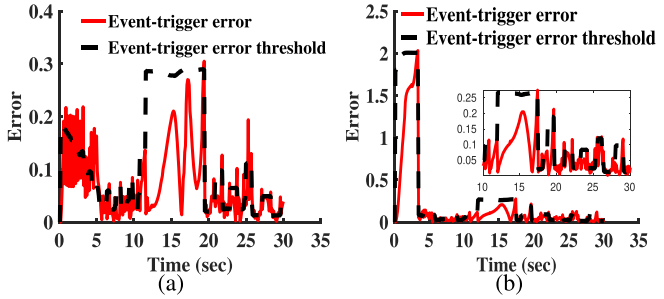

Fig. 11. Event-triggered error and threshold of (a) Follower-1 and (b) Follower-2.

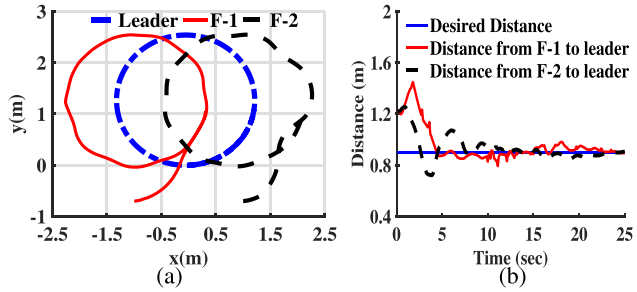

Fig. 12. (a) Trajectory of robots during circle formation. (b) Relative distance of followers from leader.

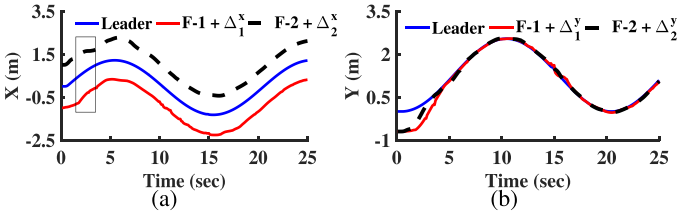

Fig. 13. (a) X-position trajectories and (b) Y-position trajectories of robots during circle formation with desired separation distance.

crossings by event-triggered error is largely reduced. The least interevent time is 0.01s.

For the validation of the proposed approach, another real-time experiment is performed with leader and follower robots trying to achieve the desired formation in the shape of "circle." The initial position of leader is $\mathrm{x}_0 = [0; 0]$. The followers are initially at $\mathrm{x}_1 = [-1; -0.7]$ and $\mathrm{x}_2 = [1; -0.7]$. The desired distance separation between leader and followers 1 and 2 should be $\Delta_1 = (0.9\,\mathrm{m}, 0\,\mathrm{m})$ and $\Delta_2 = (-0.9\,\mathrm{m}, 0\,\mathrm{m})$, respectively. The leader robot's linear velocity (v) and angular velocity (ω) is 0.2 m/s and 0.15 rad/s. The consensus parameter, system parameter, and disturbance are similar to the previous experiment.

The leader and follower robots trajectories are shown in Fig. 12(a). The leader pursues a circle-shaped trajectory with the followers following the leader trajectory maintaining a desired distance. Initially, the robots are not in consensus but after few seconds, they gradually attain the desired trajectory. Fig. 12(b) ensures that the desired separation is gradually maintained throughout the task even in the presence of disturbances.

Fig. 13 shows that the followers are achieving consensus with respect to the leader in finite time with the desired separation. The square block in Fig. 13(a) shows that the follower comes

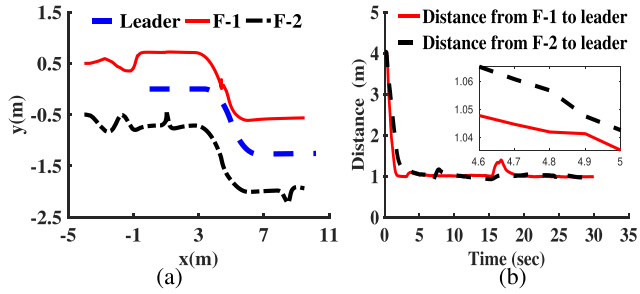

Fig. 14. Results based on [18]. (a) Trajectory of robots. (b) Relative distance of followers from leader.

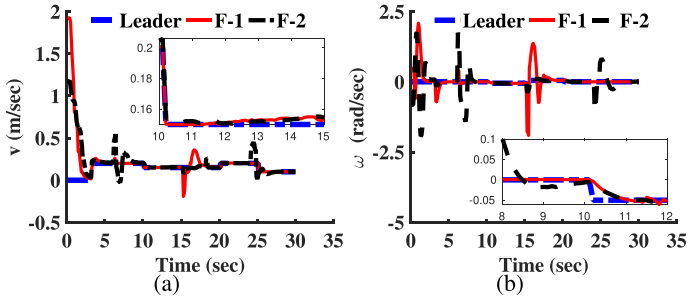

Fig. 15. Velocities based on approach in [18]. (a) Linear velocity and (b) angular velocity.

in desired formation shape and maintains a desired separation distance throughout the process with respect to the leader. It is evident from the plots that formation in MAS is achieved in finite time in the presence of time-varying matched disturbance, which infers the robustness of controller. The above experiment confirms the efficacy of the proposed approach. The consensus is achieved within 5–7 s. A YouTube link of the video for experiments with three other sets of initial positions is given in [36].

C. Comparative Analysis With Other Approaches

To compare the efficiency of the proposed approach, we have repeated the experiments for approach presented in [18]. The control law used there is defined as $u_i(t) = \gamma_i q_i^{\alpha}(t_k^i)$. The triggering condition used in [18] is $\|e_i(t)\| \leq (\eta/n^{(1-\beta)/2})^{1/\beta}\|q_i(t^i)\|^{\alpha/\beta}$, where event-triggered error magnitude is $\|e_i(t)\| = (q_i^{\alpha}(t_k^i) - q_i^{\alpha}(t^i))^{1/\beta}$. The other parameters are $\alpha \in (0, 1)$ and $\beta \in (0, 1]$. The initial position of leader is $\mathrm{x}_0 = [0\,;\,0]^T$, whereas followers are initially at $\mathrm{x}_1 = [-4\,;\,0.5]^T$ and $\mathrm{x}_2 = [-4\,;\,-0.5]^T$.

On comparing the trajectories during desired formation in Fig. 14, the proposed approach provides better trajectory than [18]. One can notice in Fig. 15 the linear and angular velocities of robots change abruptly at times for [18], whereas the change in velocities are smooth for the proposed approach. For the generalized consensus-based problem, the approach in [18] works well but not suitable for MAS with disturbance.

A comparison has been drawn out with conventional SMC approach presented in [32]. The event-triggering condition and the control law have been used as given in [32]. The robot parameters are kept the same as in this article. The trajectories

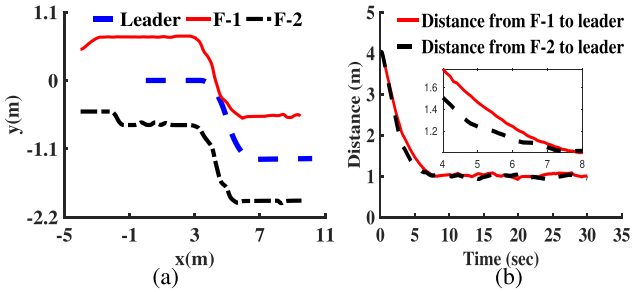

Fig. 16. Results based on [32]. (a) Trajectory of robots. (b) Relative distance of followers from leader.

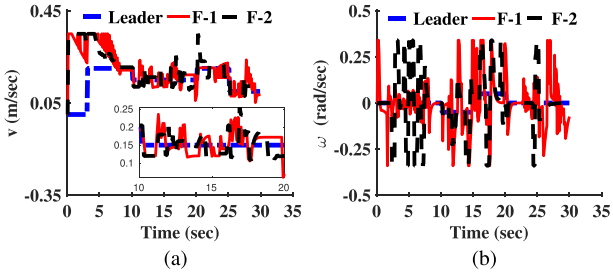

Fig. 17. Velocities based on approach in [32]. (a) Linear velocity and (b) angular velocity.

TABLE II
COMPARISON OF DIFFERENT APPROACHES

	Proposed Approach		Approach [18]		Approach [32]	
	F-1	F-2	F-1	F-2	F-1	F-2
Avg. events triggered (in %)	28.33	23.33	58.00	44.66	40.0	37.0
Min. inter-event time (in s)	0.01	0.01	0.01	0.01	0.01	0.01

F-1: Follower-1 and F-2: Follower-2.

during formation in Fig. 16 are shaky as with the linear and angular velocities in Fig. 17 too showing chattering. Though the minimum interevent time is the same for all the approaches in Table II, the average triggering is lesser for the proposed approach than the approaches in [18] and [32].

Based on the theoretical developments followed by real-time experiments, we can conclude that the proposed event-based STSMC approach is one of the best choices to handle consensus-based formation problem in the presence of disturbance.

V. CONCLUSION

This article designs a finite-time event-based STSMC for achieving consensus in a leader–follower-based MAS framework in the presence of external bounded disturbance. The proposed approach guarantees finite-time consensus of each agent along with its stability. The admissibility criteria satisfied by each agent's control update helps in avoiding the Zeno behavior during the consensus. The simulation and real-time experiments using six and three robots, respectively, for desired consensus validate the theoretical developments in the article. The results obtained justify the performance of the proposed approach to be at par with traditional time-triggered approaches and better than other existing event-based approaches. The less number of events significantly decrease the count of control updates which further reduce actuator actions, computations, and data communication required to address the problem. This ensures saving of resources available during multirobot system operation. However, this work does not consider network uncertainties among the agents. These uncertainties may be in the form of transmission delay, communication delay, packet loss, channel noise, etc. They may deteriorate the system performance from the desired objective and may even cause the system to be unstable. Another future scope of this article may be to incorporate fault tolerance in the existing model to handle the fault in the exciting model. The future work, therefore, will consider the above-mentioned aspects in the proposed approach.

REFERENCES

[1] W. Ren and R. W. Beard, *Distributed Consensus in Multi-Vehicle Cooperative Control*. London, U.K.: Springer-Verlag, 2008.
[2] Y. Toda and N. Kubota, "Self-localization based on multiresolution map for remote control of multiple mobile robots," *IEEE Trans. Ind. Inform.*, vol. 9, no. 3, pp. 1772–1781, Aug. 2013.
[3] D. Zhang, Z. Xu, H. R. Karimi, Q.-G. Wang, and L. Yu, "Distributed H_∞ output-feedback control for consensus of heterogeneous linear multiagent systems with aperiodic sampled-data communications," *IEEE Trans. Ind. Electron.*, vol. 65, no. 5, pp. 4145–4155, May 2018.
[4] H. Sayyaadi and M. Doostmohammadian, "Finite-time consensus in directed switching network topologies and time-delayed communications," *Scientia Iranica*, vol. 18, no. 1, pp. 75–85, 2011.
[5] A. Mondal, C. Bhowmick, L. Behera, and M. Jamshidi, "Trajectory tracking by multiple agents in formation with collision avoidance and connectivity assurance," *IEEE Syst. J.*, vol. 12, no. 3, pp. 2449–2460, Sep. 2018.
[6] A. Jenabzadeh and B. Safarinejadian, "Distributed tracking of nonholonomic targets over multiagent systems," *IEEE Syst. J.*, vol. 13, no. 2, pp. 1678–1681, Jun. 2019.
[7] Y. Koren and J. Borenstein, "Potential field methods and their inherent limitations for mobile robot navigation," in *Proc. IEEE Int. Conf. Robot. Autom.*, Apr. 1991, pp. 1398–1404.
[8] N. K. Dhar, N. K. Verma, and L. Behera, "Adaptive critic-based event-triggered control for HVAC system," *IEEE Trans. Ind. Informat.*, vol. 14, no. 1, pp. 178–188, Jan. 2018.
[9] A. K. Kar, N. K. Dhar, and N. K. Verma, "Event-triggered adaptive neural network controller in a cyber-physical framework," *IEEE Trans. Ind. Inform.*, vol. 15, no. 4, pp. 2101–2111, Apr. 2019.
[10] T. Henningsson, E. Johannesson, and A. Cervin, "Sporadic event-based control of first-order linear stochastic systems," *Automatica*, vol. 44, no. 11, pp. 2890–2895, 2008.
[11] A. Anta and P. Tabuada, "To sample or not to sample: Self-triggered control for nonlinear systems," *IEEE Trans. Autom. Control*, vol. 55, no. 9, pp. 2030–2042, Sep. 2010.
[12] D. V. Dimarogonas, E. Frazzoli, and K. H. Johansson, "Distributed event-triggered control for multi-agent systems," *IEEE Trans. Autom. Control*, vol. 57, no. 5, pp. 1291–1297, May 2012.
[13] A. Wang, B. Mu, and Y. Shi, "Event-triggered consensus control for multiagent systems with time-varying communication and event-detecting delays," *IEEE Trans. Control Syst. Technol.*, vol. 27, no. 99, pp. 507–515, Mar. 2019.
[14] B. Mu, K. Zhang, F. Xiao, and Y. Shi, "Event-based rendezvous control for a group of robots with asynchronous periodic detection and communication time delays," *IEEE Trans. Cybern.*, no. 99, pp. 1–10, Jul. 2018.
[15] H. Li, X. Liao, T. Huang, and W. Zhu, "Event-triggering sampling based leader-following consensus in second-order multi-agent systems," *IEEE Trans. Autom. Control*, vol. 60, no. 7, pp. 1998–2003, Jul. 2015.
[16] W. Zhu and Z.-P. Jiang, "Event-based leader-following consensus of multi-agent systems with input time delay," *IEEE Trans. Autom. Control*, vol. 60, no. 5, pp. 1362–1367, May 2015.
[17] M. Yu, C. Yan, D. Xie, and G. Xie, "Event-triggered tracking consensus with packet losses and time-varying delays," *IEEE/CAA J. Autom. Sinica*, vol. 3, no. 2, pp. 165–173, Apr. 2016.

[18] Y. Zhu, X. Guan, X. Luo, and S. Li, "Finite-time consensus of multi-agent system via nonlinear event-triggered control strategy," *IET Control Theory Appl.*, vol. 9, no. 17, pp. 2548–2552, Nov. 2015.
[19] M. Ou, H. Du, and S. Li, "Finite-time formation control of multiple nonholonomic mobile robots," *Int. J. Robust Nonlinear Control*, vol. 24, no. 1, pp. 140–165, 2014.
[20] Q. Liu, Z. Wang, X. He, and D.-H. Zhou, "Event-based *H*-infinity consensus control of multi-agent systems with relative Output feedback: The finite-horizon case," *IEEE Trans. Autom. Control*, vol. 60, no. 9, pp. 2553–2558, Sep. 2015.
[21] A. Levant, "Sliding order and sliding accuracy in sliding mode control," *Int. J. Control*, vol. 58, no. 6, pp. 1247–1263, 1993.
[22] J. A. Moreno and M. Osorio, "A Lyapunov approach to second-order sliding mode controllers and observers," in *Proc. 47th IEEE Conf. Decision Control*, Dec. 2008, pp. 2856–2861.
[23] Y. Zhang, Y. Yang, Y. Zhao, and G. Wen, "Distributed finite-time tracking control for nonlinear multi-agent systems subject to external disturbances," *Int. J. Control*, vol. 86, no. 1, pp. 29–40, 2013.
[24] S. Yu and X. Long, "Finite-time consensus for second-order multi-agent systems with disturbances by integral sliding mode," *Automatica*, vol. 54, pp. 158–165, 2015.
[25] N. Liu, R. Ling, Q. Huang, and Z. Zhu, "Second-order super-twisting sliding mode control for finite-time leader-follower consensus with uncertain nonlinear multiagent systems," *Math. Problems Eng.*, vol. 2015, pp. 1–8, 2015.
[26] H. Yang, Y. Jiang, and S. Yin, "Fault-tolerant control of time-delay markov jump systems with Itô stochastic process and output disturbance based on sliding mode observer," *IEEE Trans. Ind. Inform.*, vol. 14, no. 12, pp. 5299–5307, Dec. 2018.
[27] H. Yang and S. Yin, "Actuator and sensor fault estimation for time-delay Markov jump systems with application to wheeled mobile manipulators," *IEEE Trans. Ind. Inform.*, vol. 16, no. 5, pp. 3222–3232, May 2020.
[28] H. Yang and S. Yin, "Reduced-order sliding-mode-observer-based fault estimation for Markov jump systems," *IEEE Trans. Autom. Control*, vol. 64, no. 11, pp. 4733–4740, Nov. 2019.
[29] A. K. Behera and B. Bandyopadhyay, "Event-triggered sliding mode control for a class of nonlinear systems," *Int. J. Control*, vol. 89, no. 9, pp. 1916–1931, 2016.
[30] R. R. Nair, L. Behera, and S. Kumar, "Event-triggered finite-time integral sliding mode controller for consensus-based formation of multirobot systems with disturbances," *IEEE Trans. Control Syst. Technol.*, vol. 27, no. 1, pp. 39–47, Jan. 2019.
[31] E. Garcia, Y. Cao, and D. W. Casbeer, "An event-triggered control approach for the leader-tracking problem with heterogeneous agents," *Int. J. Control*, vol. 91, no. 5, pp. 1209–1221, 2018.
[32] A. Sinha and R. K. Mishra, "Consensus in first order nonlinear heterogeneous multi-aagent systems with event-based sliding mode control," *Int. J. Control*, vol. 93, no. 4, pp. 1–14, 2018.
[33] A. Selivanov and E. Fridman, "Event-triggered H_∞ control: A switching approach," *IEEE Trans. Autom. Control*, vol. 61, no. 10, pp. 3221–3226, Oct. 2016.
[34] A. Wang, B. Mu, and Y. Shi, "Consensus control for a multi-agent system with integral-type event-triggering condition and asynchronous periodic detection," *IEEE Trans. Ind. Electron.*, vol. 64, no. 7, pp. 5629–5639, Jul. 2017.
[35] W. Ren and N. Sorensen, "Distributed coordination architecture for multi-robot formation control," *Robot. Auton. Syst.*, vol. 56, no. 4, pp. 324–333, 2008.
[36] Finite-Time Robust Admissible Consensus Control of Multi-Robot System Under Dynamic Events. [Online]. Available: https://youtu.be/XY7LrDOX1sg

Anuj Nandanwar received the master's degree in electronics and telecommunication from the Chhattisgarh Swami Vivekanand Technical University, Bhilai, India. He is currently working toward the Ph.D. degree with the Department of Electrical Engineering, IIT Kanpur, Kanpur, India.

His research interests include cyber-physical systems, cooperative control of multirobot systems, sliding-mode control, and event-trigger control.

Narendra Kumar Dhar received the master's degree in control system from IIT Roorkee, Roorkee, India, in 2013. He is currently working toward the Ph.D. degree with the Department of Electrical Engineering, IIT Kanpur, Kanpur, India.

His research interests include cyber-physical systems, smart home automation, and softcomputing.

Dmitry Malyshev graduated from Belgorod State Technological University named after V.G. Shukhov in 2015, specializing in mechanical engineering technology.

Since 2015, he has been working at the Center for High Technologies at Belgorod State Technological University named after V.G. Shukhov. His research interests include a wide range of issues related to numerical optimization and simulation methods as applied to robots and manipulators of various structures.

Larisa Rybak graduated with honors from the Kharkov Aviation Institute, in 1985. She received the Ph.D. degree in the theory of mechanisms and machines from the Moscow Academy of Instrument Engineering, Russia, in 1992 and the Ph.D. Hab. degree in 1998.

From 1985 to 1994, she worked with the Moscow State Open University as an Assistant Professor. From 1994 to 2002, she worked with the Mechanical Engineering Research Institute of the Russian Academy of Sciences. Since 2004, she has been working with the Belgorod State Technological University, named after V.G. Shukhov, as a Professor and Head of the Scientific Laboratory of Mechatronics and Robotics. Her research interests include mechanics of machines and robots, intelligent control systems for machines and robots, mathematical simulation, optimization, and computational methods.

Laxmidhar Behera (Senior Member, IEEE) received the B.Sc. and M.Sc. degrees in engineering from, NIT Rourkela, Rourkela, India, in 1988 and 1990, respectively, and the Ph.D. degree from IIT Delhi, New Delhi, India, in 1996. He pursued the postdoctoral studies in the German National Research Center for Information Technology, GMD, Sank Augustin, Germany from 2000–2001.

From 1995 to 1999, he has worked as an Assistant Professor with BITS Pilani and as a Reader with Intelligent Systems Research Center, University of Ulster, UK, form 2007 to 2009. He has also worked as a Visiting Researcher/Professor with FHG, Germany, and ETH, Zurich. He is currently working as Poonam and Prabhu Goel Chair Professor with IIT Kanpur, Kanpur, India, having research and teaching experience of more than 24 years. His primary research interests include the convergence of machine learning, control theory, robotic vision and heterogeneous robotic platforms. His other research interests include intelligent control, semantic signal/music processing, neural networks, control of cyber-physical systems and cognitive modelling.

Dr. Behera has established industrial collaboration with TCS, Renault Nissan, BEL, Bangalore and ADNOC, Abu Dhabi. He is a Fellow of INAE.